AIAA 2000-1525
Detection and Correction of Poorly Converged Optimizations by Iteratively Reweighted Least Squares

H. Kim, W. H. Mason, L. T. Watson and B. Grossman
Virginia Polytechnic Institute and State University,
Blacksburg, VA

and

M. Papila and R.T. Haftka
University of Florida
Gainesville, FL

41st AIAA/ASME/ASCE/AHS/ASC Structures, Structural Dynamics, and Materials Conference
3-6 April 2000 / Atlanta, GA

AIAA-2000-1525

DETECTION AND CORRECTION OF POORLY CONVERGED OPTIMIZATIONS BY ITERATIVELY REWEIGHTED LEAST SQUARES

Hongman Kim*, Melih Papila†, William H. Mason‡, Raphael T. Haftka§, Layne T. Watson¶, and Bernard Grossman**
Multidisciplinary Analysis and Design (*MAD*) *Center for Advanced Vehicles*
Virginia Polytechnic Institute and State University
Blacksburg, VA 24061-0203

Abstract

The use of Iteratively Reweighted Least Squares (IRLS) for detecting design points where structural optimizations give poor designs is demonstrated. Since most optimization error is one sided with poor results producing an overweight objective value, a nonsymmetrical version of IRLS (NIRLS) that takes into account the asymmetry in optimization errors is also developed. Optimization studies with various sets of convergence criteria on wing bending material weight of a high speed civil transport are used to demonstrate these techniques. First, inspection of poor designs by a visualization technique that plots objective function and constraint boundaries on planes including the suspected points, indicated that poor results were due to incomplete convergence of the optimization procedure rather than due to local minima. Results obtained with several hundred design points indicated that IRLS techniques can find most of the points with large optimization errors, but that NIRLS techniques are much more reliable in this task. Finally, the paper shows that the choice of convergence settings and parameters can have large effects on optimization errors. In particular, tighter criteria for some parameters may actually increase optimization error.

* Graduate Research Assistant, Department of Aerospace and Ocean Engineering, Student Member AIAA.
† Graduate Research Assistant, Department of Aerospace Engineering, Mechanics and Engineering Science, University of Florida, Gainesville, FL, Student Member AIAA.
‡ Professor, Department of Aerospace and Ocean Engineering, Associate Fellow AIAA.
§ Distinguished Professor, Department of Aerospace Engineering, Mechanics and Engineering Science, University of Florida, Gainesville, FL, Fellow AIAA.
¶ Professor, Departments of Computer Science and Mathematics.
** Professor and Department Head, Department of Aerospace and Ocean Engineering, Associate Fellow AIAA.

1. Introduction

Optimization procedures often produce poor results due to algorithmic difficulties, software problems, or local optima. When a single optimization is flawed, it may be difficult to detect the problem, because the ill conditioning responsible for the problem may make it difficult to apply optimality criteria unambiguously. However, in many applications a large number of optimizations are performed for a range of problem parameters. For example, our research group routinely performs thousands of structural optimizations of wing structures for the purpose of developing equations that predict wing structural weight as a function of the aerodynamic shape of the wing[1]. When such multiple optimizations are available, statistical analysis can be done to detect incorrect optimal results. For example, Papila and Haftka[2] used iteratively reweighted least squares[3, 4] (IRLS) to detect such points, called outliers. They corrected the data by re-optimization from slightly different starting points or by switching optimization algorithms.

One important observation about the outlier points (incorrect computed optima) is that they are consistently heavier designs than the true optimal designs. That is, the optimization error has positive bias. There are two implications of this bias in the optimization error. First, we expect that the incorrect optimal will be lowered by correction efforts. Second, the symmetric weighting function used in IRLS procedures can be improved by taking into account the error bias. One objective of this paper is to demonstrate this approach of using nonsymmetrical weighting functions in an IRLS procedure for detecting outliers. The procedure is demonstrated on structural optimization of wing box material for various aerodynamic configurations of a high-speed civil transport.

Poor optimization results may be the result of local optima or of premature convergence of the optimization

procedure. We use visualization of the design space along selected planes, as suggested by Knill et al.[5], to tell whether we have one case or the other. In most cases we have found that poor results are caused by premature convergence due to the choice of the convergence criteria in the optimization procedure. A second objective of this paper is to demonstrate the usefulness of outlier detection for discovering the poor choice of parameters, and for estimating the magnitude of the resulting errors.

2. Iteratively Reweighted Least Squares

The standard least squares procedure for response surface estimation[6] is not robust with respect to bad data. Robust regression methods have been developed which give reasonable estimates even if the data is contaminated with outliers (bad data). In addition, robust regression[7] can locate the outliers, allowing us to examine the outliers and try to correct them whenever possible.

To describe the robust regression method (known as M-estimation) used here, we first consider the standard linear regression model. With n data points and p parameters in the regression model, the linear regression model is

$$y = X\beta + \varepsilon \tag{1}$$

where X is a $n \times p$ Gram matrix of the shape functions used in the model (typically monomials), β is a p-vector of coefficients to be estimated and ε is an n-vector of random errors. For a robust estimate β, we minimize a measure of the residuals r_i:

$$e(\beta) = \sum_{i=1}^{n} \rho(r_i), \quad \text{where} \quad r_i = \frac{(y - X\beta)_i}{\sigma}. \tag{2}$$

Here, ρ is a function of the residual scaled by σ, a known estimate of the standard deviation of ε. For example, in the case of the familiar least squares method, $\rho(s) = s^2/2$. A necessary condition for a minimum is

$$\nabla e(\beta) = 0. \tag{3}$$

If we define $\psi(s) = d\rho(s)/ds$, then a necessary condition for a minimum becomes

$$X^T \Psi = 0, \tag{4}$$

where $\Psi = (\psi(r_1), \psi(r_2), \ldots, \psi(r_n))^T$. Defining the weight function $w(s) = \psi(s)/s$, (4) becomes

$$X^T W(r) r = 0 \tag{5}$$

where $W(r) = diag(w(r_1), w(r_2), \ldots, w(r_n))$. Note that for ordinary least squares $\psi(s) = s$ and $w(s) = 1$.

For ordinary least squares, (5) is a linear equation for the coefficient vector β. However, in general (5) is a system of nonlinear equations and iterative methods are required. The most popular approach is iteratively reweighted least squares (IRLS), which is attributed to Beaton and Tukey[3]. Rewriting the necessary condition as

$$X^T W(r) X\beta = X^T W(r) y, \tag{6}$$

the iterative formula can be written as

$$\beta^{(i+1)} = \left[X^T W\left(\frac{y - X\beta^{(i)}}{\sigma}\right) X \right]^{-1} X^T W\left(\frac{y - X\beta^{(i)}}{\sigma}\right) y, \tag{7}$$

or,

$$\beta^{(i+1)} = \beta^{(i)} + \left[X^T W\left(\frac{y - X\beta^{(i)}}{\sigma}\right) X \right]^{-1} X^T W\left(\frac{y - X\beta^{(i)}}{\sigma}\right) \left(y - X^{(i)}\right). \tag{8}$$

Several possible weight functions were considered here, summarized in Table 1 and Fig. 1. We preferred Beaton and Tukey's biweight function[3] to Huber's minimax[8] because it gives zero weight to the outliers and thus the outliers are clearly detected. The two other functions, NIRLS1 and NIRLS2, will be discussed later. An estimate of σ was calculated as $1.5 \cdot median(|y_i - \mathbf{x}_i\beta|)$ as recommended by Myers[9]. B is a tuning constant depending on the characteristics of the noise distribution. Myers[9] suggested limiting the tuning constant to a range of one to three. The shape of the weight functions in Fig. 1 clearly shows that they penalize outliers with zero or low weight while giving a weight of one or near one, to inliers. Equations (7) is a fixed point iteration and is not guaranteed to converge to the global minimum of $e(\beta)$. Because the IRLS results depend on the initial guess for β, we need a good initial guess of the regressor coefficients. With a nonredescending ψ function (Figure 2) like Huber's minimax, Birch[10] proved that (7) is globally convergent to a unique solution, the global minimum of $e(\beta)$. Therefore, we adopted Huber's minimax function to get the initial estimates of the regressor coefficients. Then the IRLS procedure using the biweight function was computed using these initial coefficients.

The usual IRLS procedure assumes no bias of the residual sign. However, for wing structural weight minimization, the residual $r_i = (y - X\beta)_i/\sigma$ is mostly positive for outliers because they are mostly caused by optimization failure and are consequently heavier. In order to account for the bias in the outliers, we modified the shape of the weight function. We tried two asymmetric weight functions, derived from Beaton and Tukey's biweight, and labeled them as NIRLS (Nonsymmetrical IRLS) weight functions. For NIRLS1

negative residuals have a weight of one, assuming the points are good, while positive residuals are weighted by the biweight function. However, because NIRLS1 does not downweight large negative residuals, the estimated β can be susceptible to outliers due to modeling error (true function different from the assumed response surface model). Therefore, we devised NIRLS2 as a compromise between the biweight and NIRLS1 (Fig. 1). NIRLS2 downweights points with negative residual less than IRLS, but it gives zero weight if the negative error is greater than a given limit.

3. Description of the HSCT Design Problem

The problem studied in this paper is a 250 passenger HSCT design with a 5500 n.mi. range and cruise speed of Mach 2.4. A general HSCT model[1, 11, 12] developed by the Multidisciplinary Analysis and Design (MAD) Center for Advanced Vehicles at Virginia Tech includes 29 configuration design variables. Of these, 26 describe the geometry, two the mission, and one the thrust (Table 2). Following Balabanov et al.[1], our objective is to fit a response surface to optimal wing bending material weight (W_b) from structural optimization as a function of configuration design variables. There are four load cases for the HSCT design study that represent different points on the flight envelope.

We applied the method to simplified versions of the HSCT design problem with only five configuration variables. Version A, Table 2 (a), selected five variables defining the wing planform, including root chord c_{root}, x-coordinate of the leading edge break point *LEbx*, y-coordinate of the leading edge break point *LEby*, x-coordinate of the leading edge at the wing tip *LEtx*, and wing semi span *b/2*. Version B, Table 2 (b), following Knill et al.[5] includes root chord c_{root}, tip chord c_{tip}, inboard leading edge sweep angle Λ_{ILE}, thickness to chord ratio for the airfoil *t/c*, and the fuel weight, W_{fuel}. Figure 3 illustrates the design variables of the two HSCT design problems. Other variables, such as fuselage, vertical tail, mission, and thrust related parameters, are kept unchanged at the baseline values for both versions.

In this study, a structural optimization procedure based on finite element analysis using GENESIS[13] was applied. The finite element model, developed by Balabanov[1], uses 40 design variables, including 26 variables to control skin panel thickness, 12 variables to control spar cap areas, and two for the rib cap areas. The HSCT codes[11, 12] calculate aerodynamic loads for each of the four load cases, and a mesh generator by Balabanov[1] calculates the FEM mesh and applied load at the structural nodes, and creates the input for GENESIS. The structural optimization is performed for each aircraft configuration. The objective function is the total wing structural weight and the wing bending material weight W_b is calculated from the optimal structural design.

4. Test Problem Study of Optimization Failure: Rosenbrock Function in Five Dimensions

Before addressing the HSCT problem, it is worthwhile to illustrate our premise using a simple test problem. It is not unusual that an optimization code fails to find even a local optimum. This may happen due to ill conditioning of the design space, and it is difficult for users to detect the failure of the optimization procedure. Here we will demonstrate the failure of some optimization algorithms for a simple unconstrained minimization problem, the generalized Rosenbrock function[14] in five dimensions:

$$f(x) = \sum_{k=1}^{n-1} 100(x_{k+1} - x_k^{\,2})^2 + (1 - x_k)^2 \qquad (9)$$

The unconstrained minimization problem has the unique solution $x^* = (1, 1, 1, 1, 1)$ at which $f^* = 0$. We performed 500 runs from different initial points that were randomly generated. For the purpose of this demonstration we used DOT[15], Matlab[16], and a trust region routine from the PORT[17, 18] library with finite difference gradients. The results are summarized in Table 3. Matlab failed to find the true optimum in seven out of 500 runs. DOT failed in 27 out of 500 runs, but that number was reduced to 4 when the scaling of the design variables was turned off. All failures occurred at essentially the same point. The condition number of the Hessian matrix at the point was about 2400. The trust region algorithm[19], implemented in PORT library, known to have a more robust convergence criterion, failed, 180 out of 500 cases, converging to various points. This unexpected failure was traced to poor estimation of gradients. Yet, when analytical gradients were provided, the trust region algorithm had no failures. In contrast, no noticeable improvements were achieved by analytical gradients with DOT or Matlab. This example shows that the performance of numerical optimization depends on the algorithms adopted and detailed options used.

5. Visualization to Check of the Soundness of an Optimum

When the solution is not known as in practical applications of nonlinear programming, we have to use various aids to detect optimization failure. Here we consider structural optimization results for the HSCT. We generated 121 design points using an orthogonal array[20] experimental design in the five dimensional space of the HSCT problem Version A. The 15th design point,

denoted #15, identified as an outlier, was selected for further study, since we could achieve a 26.6% of reduction of W_b with four additional GENESIS runs starting from different initial design points. We used a design space visualization to determine the nature of the optimization failure. We started by checking whether there were better designs near #15 by analyzing100 design points with the 40 structural design variables perturbed ±1% randomly from their values at #15. Six of the 100 points were feasible points better than #15.

In order to visualize the neighborhood of #15, two better feasible points were selected, the 35th and 64th perturbed points, denoted as #15P35 and #15P64. To visualize the design space, a grid of points in a plane passing through #15, #15P35, and #15P64, was analyzed. Figure 4 shows contours of the objective function increment, normalized to the value at #15, and the constraint boundaries in the plane. The feasible points are shown as empty circles and filled circles are infeasible points on the grid. We observe that point A is the best feasible point in the plane and there is no constraint barrier between #15 and point A. This shows that #15 represents optimization failure, and illustrates the value of this visualization technique.

6. Effects of Code Parameters on Optimization Error

The optimization error depends on many convergence parameters, called control parameters in GENESIS. This section presents the results of a study illustrating how the choice of control parameters affects the results. The control parameters can be categorized into move limit parameters, convergence criteria and inner optimization control parameters (Table 4). There are two loops in the GENESIS[21] (Figure 5). The outer loop performs detailed FEM analysis of the structure and creates, in order to reduce the number of expensive FEM analysis, approximations of the original structural optimization problem. Move limits are imposed to restrict the approximate optimization to the region where the approximation is valid. The outer loop passes the approximate optimization problem to the inner loop where the actual optimization is carried out. The approximation and optimization is continued until no further change of design variables, called soft convergence, or no further change of the objective function, called hard convergence. Optimization parameters affect the performance of optimization, quality of the optimization results and the computational cost.

Experimental design points on which response surfaces are fit are generated to cover the design space. Two different experimental designs were used for the two five variable HSCT problems; for Version A, we used 121 orthogonal array design points, and for Version B, a mixed experimental design[2] of 126 points that included centered composite design and orthogonal array design was used. GENESIS structural optimizations using different sets of parameters were performed for each set. Table 4 lists the description of parameters and the actual values used in this study. Case 1 uses the default parameters provided by GENESIS. Case 2 is the same as Case 1 except that the parameter ITRMOP was increased from 2 to 5. ITRMOP controls the convergence of the inner optimization. For the approximate optimization to converge, the inner loop convergence criterion on the objective function change must be satisfied for ITRMOP consecutive times. After extensive experimentation with the optimization parameters and help from the developers of GENESIS, we found that this parameter was the most important for improving the accuracy of the optimization for our problem.

Case 3 employs tighter move limits and convergence criteria than Case 1. It reflects our first attempt to improve the optimization results. Case 4 is the same as Case 3 except that ITRMOP is 5. Case 7 employs moderately tight parameters, which was frequently adopted in our HSCT design problem. Case 8 is the same as Case 7 except that ITRMOP is 5. Case 5 will be discussed later. Parameters from Case 1 to Case 5 were tested on Version A, and Case 1, Case 2, Case 7, and Case 8 were tested on Version B of the HSCT design problem. The values of the control parameters for each case are given in Table 4. Table 5 shows the mean improvements of W_b with respect to the default parameters of Case 1, when using parameters from Case 2 to Case 5. It is seen that tightening the convergence criteria for ITRMOP=2 (Case 3) actually had a detrimental effect. The effect of ITRMOP=5 in Case 2, was an improvement of about 692.5 lbs., which is about 1.5% of the average of W_b.

The numerical noise due to errors in the structural optimization can be visualized by plotting the optimum W_b along a straight line connecting two points in the HSCT design space. If we denote the two end points as x_0 and x_1, Figure 6 (a) is a design line plot of W_b at $x = (1-\alpha)x_0 + \alpha x_1$ in the HSCT design space of Version A. The biased noise in Case 3 is serious while Case 1 has a reasonable level of noise. Case 4 results are almost identical to Case 2. Figure 6 (b), a design line plot for Version B, shows similar effects of optimization parameters; moderately tight parameters in Case 7 had detrimental effects compared to the default parameters, but the increased ITRMOP removed most of the noise in the data. In both versions of the problem, we see clearly that poor optima produce heavier results.

Table 5 also provides the computational cost associated with the various options. It is seen that the cost associated with ITRMOP=5 is substantial, ranging from a 59% increase for Case 2 to 148% for Case 4. This

may explain why ITRMOP=2 is the default value in GENESIS.

In addition, we tested another optimization setup, Case 5 in Table 4. The intention of introducing Case 5 was to find which categories of parameters caused the very bad performance in Case 3. Only convergence criteria are tightened in Case 5, while keeping the move limits at the default values. We can see in Table 5 that Case 5 achieved 0.5% improvement compared to Case 1. Case 3 that has tightened move limits compared to Case 5, resulted in worse W_b results. Therefore, we can conclude that the tight move limits caused the poor optimization with Case 3. Tightening the move limits without increasing ITRMOP, increased the chance of premature convergence.

7. Detection and Correction of Poor Optimization by IRLS and NIRLS

The IRLS procedure to identify poor optimizations was applied to the lower fidelity optimization data, Case 1 and Case 3 in the Version A and Case 1 and Case 7 in the Version B of the HSCT problem. A full quadratic model was used and the IRLS/NIRLS outlier detection was tried using the SAS statistical software[22]. Two different values of B, 1.9 and 1.0, were used to check the effects of the tuning constant, which acts like a threshold for outlier detection (Table 1). A smaller B leads to a more aggressive outlier search. The allowable region around the response surface for good points becomes narrower, and more points will be declared outliers. From the results of the previous section, we have multiple W_b data from different optimization settings. For Version A, we estimated true W_b on the 121 experimental design points by taking the best of four W_b's from Case 1 to Case 4. Similarly, for the Version B, we estimate the true W_b as the minimum of Case 1, Case 2, Case 7, and Case 8. We tried to correct the detected outliers by the estimated true values. Full quadratic response surfaces were fit to the data before and after correction to measure the noise level remaining in the data. We also expect to improve the prediction accuracy of response surfaces by outlier correction.

Results for Version A

Table 6 presents a summary of the outlier detection and correction results for the wing bending material weight data for Case 1, W_{b1} with IRLS and NIRLS. Outliers detected were repaired by repeating the optimization with ITRMOP=5. In order to assess the success in detection, all 121 points were also repaired, and the results are shown in the last row in Table 6.

With a tuning constant B=1.9, IRLS identified 14 data points as outliers while 19 and 18 data points were found by NIRLS1 and NIRL2, respectively. The actual magnitude of error of the outliers can be calculated by comparing W_{b1} to the repaired value. Thirteen out of the 14 outliers by IRLS had nonzero improvements. The average correction of outliers was 2940 lbs. compared to 414 lbs for inliers. However, the very large outliers are of particular concern. We defined large outliers as those showing 10% or greater relative error. Two out of 121 points satisfy this criterion. These were detected by all options except for IRLS with B=1.0.

Figure 7 shows the actual error (i.e., W_b correction) distribution of both of the detected outliers and inliers versus w, the weight in IRLS. Figure 7 (a) shows that IRLS left many moderate outliers undetected. By more aggressive detection with B=1.0, IRLS declared 45 points as outliers and Figure 7 (b) shows that more of the moderate outliers were newly found by decreasing B. However, only one of the two big outliers was detected by IRLS despite of the reduced tuning constant.

Quadratic response surfaces were fit to the original and repaired Case 1 data. Before repair, the root mean square error (RMSE) was 6.5% of the mean W_b. and this was reduced only slightly to 6.2% by repair. This small gain indicates that most of the RMSE is due to modeling error, reflecting the inadequacy of quadratic polynomial.

Table 7 and Fig. 8 show results for Case 3, which contains 33 big outliers. The advantage of NIRLS over IRLS is clearly demonstrated by comparing the results when B=1.0. NIRLS successfully detected almost all big and many moderate outliers, while IRLS missed almost half of the big outliers. With a larger amount of noise, the RMSE of the quadratic response surface on W_{b3} was reduced from 9.5% to 6.2% by NIRLS repair with B=1.9. There was little further improvement of RMSE with B=1.0, although more outliers are repaired. This implies that outliers with large errors have dominant effects on the predictive accuracy of response surfaces.

Figure 9 compares the response surfaces before and after repair on the design line of Fig. 6. The response surfaces based on the uncorrected W_{b3} over-predicted the response in the right half of the plot. For B=1.9, as shown in Figure 9 (a), the response surface based on repair by IRLS was improved. Note that the response surface from NIRLS1 repair lies on top of that of IRLS. However, Figure 9 (b) indicates that NIRLS1 repair was better than IRLS with B=1.0 as expected from the results of Table 7.

Results for Version B

Table 8 shows results for Case 1. The number of big outliers for this case, 12, is much larger than for Version A, indicating a much higher level of noise. This may reflect the use of vertex points, at the far reaches of the design domain, where unusual configurations are more prone to optimization difficulties. Table 8 indicates that the NIRLS procedures were again more successful than IRLS in identifying the big outliers. Also the ratio of

correction weight for outliers and inliers is much better for the NIRLS procedures, indicating that they are more successful in homing in on points with large errors. This time, with more noise, all procedures produced substantial reduction in RMSE. The IRLS procedure did slightly better than the NIRLS, something for which we do not have an explanation.

Table 9 shows results for Case 7, which like Case 3 has substantially more noise than Case 1. The number of big outliers is 34, and again, the NIRLS procedures are much more successful than the IRLS procedure in finding most of these outliers, especially with the aggressive search corresponding to B=1. As in Table 8, the IRLS procedure does slightly better in terms of RMSE reduction.

Taken together, the results for both versions indicate that IRLS procedures are useful for detecting points with large optimization errors, and that the NIRLS procedures are substantially more reliable in this task, especially under conditions of aggressive search. While RMSE errors are not influenced much by the choice between IRLS and NIRLS, Fig. 9 indicates that prediction errors may improve with the NIRLS procedure.

8. Concluding Remarks

Response surface techniques provide statistical tools to identify outliers in the data that do not fit the underlying model. We have demonstrated the use of one of these tools, Iteratively Reweighted Least Squares (IRLS) for detecting design points where structural optimization gave poor designs. Since optimization error is one sided, we have also proposed a nonsymmetrical version of IRLS (NIRLS) that takes into account the asymmetry in optimization errors.

Optimization studies with various sets of convergence criteria on wing bending material weight of a high speed civil transport (HSCT) were used to demonstrate the usefulness of the techniques. First, some of the points detected by IRLS and NIRLS were inspected by a design space visualization technique that plots objective function and constraint boundaries on planes including the suspect design points. The visualization indicated that poor results were due to incomplete convergence of the optimization procedure rather than due to local minima.

Next, all the points used for the construction of the response surface were repaired by re-optimizing them with the best set of convergence criteria at our disposal. This allowed us to check how successful the IRLS and NIRLS procedures were in detecting outliers. We focused mostly on big outliers, where the error in optimal weight was more than 10%. We found that the NIRLS procedures were much more reliable in detecting these big outliers. While there was not much difference between the different procedures in terms of reducing rms error in the response surface, there was some indication that the response surfaces based on NIRLS repair may have smaller prediction errors.

Finally, the study revealed that convergence setting can have large effects on optimization errors. In particular, we found that tighter criteria for some parameters may actually increase optimization error.

Acknowledgement

The work of Papila and Haftka at the University of Florida was supported by NASA grant NAG1-2177, and the work at Virginia Tech was partially supported by NSF grant DMI-997911.

References

1. Balabanov, V., Giunta, A. A., Golovidov, O., Grossman, B., Mason, W. H., Watson, L. T., and Haftka, R. T., "Reasonable Design Space Approach to Response Surface Approximation," *Journal of Aircraft*, Vol. 36, 1999, pp. 308-315.
2. Papila, M. and Haftka, R. T., "Uncertainty and Wing Structural Weight Approximations," AIAA Paper 99-1312, 40th AIAA/ASME/ASCE/ASC Structures, Structural Dynamics, and Material Conference, St. Louis, MO, April 1999.
3. Beaton, A. E. and Tukey, J. W., "The Fitting of Power Series, Meaning Polynomials, Illustrated on Band-Spectroscopic Data," *Technometrics*, Vol. 16, 1974, pp. 147-185.
4. Holland, P. H., and Welsch, R. E., "Robust Regression Using Iteratively Reweighted Least Squares," *Communications in Statistics: Theory and Methods*, Vol. 6, 1977, pp. 813-827.
5. Knill, D.L., Giunta, A. A., Baker, C.A., Grossman, B., Mason, W. H., Haftka, R. T., and Watson, L. T., "Response Surface Models Combining Linear and Euler Aerodynamics for Supersonic Transport Design," *Journal of Aircraft*, Vol. 36, No. 1, 1999, pp. 75-86.
6. Myers, R. H., and Montgomery, D. C., *Response Surface Methodology: Process and Product Optimization Using Designed Experiments*, John Wiley and Sons, New York, N. Y., 1995.
7. Rousseuw, P. J. and Leroy, A. M., *Robust Regression and Outlier Detection*, Wiley, NY., 1987.
8. Huber, P. J., "Robust Estimation of a Location Parameter," *Annals of Mathematical Statistics*, Vol. 35, 1964, pp.73-101.
9. Myers, R. H., *Classical and Modern Regression with Applications*, PWS-KENT, Boston, 1990.

10. Birch, J. B., "Some Convergence Properties of Iteratively Reweighted Least Squares in the Location Model," *Communications in Statistics: Simulation and Computation*, Vol. 9, 1980, pp. 359-369.
11. Giunta, A. A., Balabanov, V., Burgee, S., Grossman, B., Haftka, R. T., Mason, W. H., and Watson, L. T., "Multidisciplinary Optimisation of a Supersonic Transport Using Design of Experiments Theory and Response Surface Modelling," *Aeronautical Journal*, Vol. 101, No. 1008, 1997, pp. 347-356.
12. Baker, C. A., Grossman, B., Haftka, R. T., Mason, W. H., and Watson, L. T., "HSCT Configuration Design Space Exploration Using Aerodynamic Response Surface Approximations," Proceedings of the 7th AIAA/NASA/ISSMO Symposium on Multidisciplinary Analysis and Optimization, Paper No. 98-4803-CP, St. Louis, MO, Sept. 1998, pp. 769-777.
13. VMA Engineering, *GENESIS User Manual*, Version 5.0, Colorado Springs, CO, 1998.
14. Schittkowski, K., *More Test Problems for Nonlinear Programming Codes, Lecture Notes in Economics and Mathematical Systems*, Vol. 282, Springer-Verlag, Berlin, 1987, pp. 118-123.
15. Vanderplaats Research & Development, Inc., *DOT Design Optimization Tools Users Manual*, Colorado Springs, CO, 1995.
16. Math Works, Inc., *Matlab Optimization Toolbox Users Guide*, Version 5, Natick, MA, 1997.
17. Gay, D. M., "Subroutines for Unconstrained Minimization Using a Model/Thrust-Region Approach," *ACM Transactions on Mathematical Software*, Vol. 9, No. 4, December, 1983, pp.503-512.
18. Gay, D. M., http://www.bell-labs.com/projects/PORT
19. Dennis, J. E., Jr., and Schnabel, R. B., *Numerical Methods for Unconstrained Optimization and Nonlinear Equations*, Prentice Hall, Englewood Cliffs, NJ, 1983.
20. Bose, R. C., "On the Application of the Properties of Galois Fields to the Problem of Construction of Hyper-Graeco-Latin Squares," *Sankhya* (*The Indian Journal of statistics*), Vol. 3, 1938, pp. 323-338.
21. Vanderplaats, G. N., and Miura, H., "GENESIS-Structural Synthesis Software Using Advanced Approximation Techniques," AIAA Paper 92-4839, 4th AIAA/USAF/NASA/OAI Symposium on Multidisciplinary Analysis and Optimization, Cleveland, OH, Sep 1992.
22. SAS Institutes, Inc., *SAS Users Guide*, Version 6, Fourth Edition, 1990.

Table 1: Weight functions.

Name	$W(r)$	Range	Tuning Constant
Huber's minimax	1 $H\|r\|^{-1}$	$\|r\| \le H$ $\|r\| > H$	H=1.0
Beaton and Tukey's biweight	$(1-(r/B)^2)^2$ 0	$\|r\| \le B$ $\|r\| > B$	B=1.0 ~ 1.9
NIRLS1	1 $(1-(r/B)^2)^2$ 0	$r \le 0$ $0 < r \le B$ $r > B$	B=1.0 ~ 1.9
NIRLS2	0 $(1-(r/(2B))^2)^2$ $(1-(r/B)^2)^2$ 0	$r \le -2B$ $-2B < r \le 0$ $0 < r \le B$ $r > B$	B=1.0 ~ 1.9

Table 2 (a): Configuration design variables for HSCT with corresponding values and ranges (5 variable Version A).

Name of design variables	**Value of design variable**
Planform Variables	
Wing root chord, c_{root}	156 - 211 ft
LE break point, x, $LEbx$	99.3 – 134.4 ft
LE break point, y, $LEby$	35.3 – 47.8 ft
TE break point, x, $TEbx$	(= $LEbx$+0.25 c_{root})
TE break point, y, $TEby$	(= $LEby$)
LE wing tip, x, $Letx$	120.6 – 163.2 ft
Wing tip chord, c_{tip}	10.2 ft
Wing semi span, $b/2$	61.4 – 83.1 ft
Airfoil Variables	
Location of max. thickness, $(x/c)_{max\text{-}t}$	0.49
LE radius, R_{LE}	2.94
Thickness to chord ratio at root, $(t/c)_{root}$	2.32 %
Thickness to chord ratio LE break, $(t/c)_{break}$	1.73 %
Thickness to chord ratio at tip, $(t/c)_{tip}$	1.50 %
Fuselage Variables	
Fuselage restraint 1 location, x_{fus1}	2.75 ft
Fuselage restraint 1 radius, r_{fus1}	0.628 ft
Fuselage restraint 2 location, x_{fus2}	14.4 ft
Fuselage restraint 2 radius, r_{fus2}	2.48 ft
Fuselage restraint 3 location, x_{fus3}	114 ft
Fuselage restraint 3 radius, r_{fus3}	5.60 ft
Fuselage restraint 4 location, x_{fus4}	178 ft
Fuselage restraint 4 radius, r_{fus4}	5.53 ft
Nacelle, Mission, and Empennage Variables	
Inboard nacelle location, $y_{nacelle}$	7.05 ft
Distance between nacelles, $\Delta y_{nacelle}$	14.4 ft
Fuel weight, W_{fuel}	386666 lb
Starting cruise altitude	58948 ft
Cruise climb rate	37.4 ft/min
Vertical tail area	443.8 ft^2
Horizontal tail area	729.9 ft^2
Engine thrust	48657 lb.

Table 2 (b): Configuration design variables for HSCT with corresponding values and ranges (5 variable Version B).

Design Variable	Value of design variable
Planform Variables	
Root chord, c_{root}	150 – 190 ft
Tip chord, c_{tip}	7 – 13 ft
Wing semi-span, *b/2*	74 ft
Length of inboard LE, s_{ILE}	132 ft
Inboard LE sweep, Λ_{ILE}	67° – 76°
Outboard LE sweep, Λ_{OLE}	25°
Length of inboard TE, s_{ITE}	Straight TE
Inboard TE sweep, Λ_{ITE}	Straight TE
Airfoil Variables	
Location of max. thickness, $(x/c)_{max\text{-}t}$	40%
LE radius, R_{LE}	2.5
Thickness to chord ratio at root, $(t/c)_{root}$	1.5 – 2.7%
Thickness to chord ratio LE break, $(t/c)_{break}$	$(t/c)_{break}=(t/c)_{root}$
Thickness to chord ratio at tip, $(t/c)_{tip}$	$(t/c)_{tip}=(t/c)_{root}$
Fuselage Variables	
Fuselage restraint 1 location, x_{fus1}	50 ft
Fuselage restraint 1 radius, r_{fus1}	5.2 ft
Fuselage restraint 2 location, x_{fus2}	100 ft
Fuselage restraint 2 radius, r_{fus2}	5.7 ft
Fuselage restraint 3 location, x_{fus3}	200 ft
Fuselage restraint 3 radius, r_{fus3}	5.9 ft
Fuselage restraint 4 location, x_{fus4}	250 ft
Fuselage restraint 4 radius, r_{fus4}	5.5 ft
Nacelle, Mission, and Empennage Variables	
Inboard nacelle location, $y_{nacelle}$	20 ft
Distance between nacelles, $\Delta y_{nacelle}$	6 ft
Fuel weight, W_{fuel}	280000 – 350000 lb.
Starting cruise altitude	65000 ft
Cruise climb rate	100 ft/min
Vertical tail area	548 ft^2
Horizontal tail area	No horizontal tail
Engine thrust	39000 lb.

Table 3: Failure of optimizer in 5 dimensional Rosenbrock function.

	Matlab	DOT		PORT	
Algorithm	BFGS	BFGS	BFGS (DV scaling off)	Trust region (Finite difference gradient)	Trust region (Analytic gradient)
Number of failure out of 500 runs	7	27	4	180	0

Table 4: Optimization control parameters used in GENESIS.

Category	Name of Parameter	Description	Case 1	Case 2	Case 3	Case 4	Case 5	Case 7	Case 8
Move Limits	DELP	Fractional change allowed for properties	0.5		0.02		0.5	0.5	
	DPMIN	Minimum move limit for properties	0.1		0.1E-4		0.1	0.1E-4	
	DELX	Fractional change allowed for design variables	0.5		0.05		0.5	0.5	
	DXMIN	Minimum move limit for design variables	0.1		0.1E-4		0.1	0.1E-4	
	REDUC1	To multiply all the move limits by this number if internal approximate problem is NOT doing well	0.5		0.9		0.5	0.5	
	REDUC2	To divide all the move limits by this number if internal approximate problem is doing well	0.75		0.9		0.75	0.75	
Hard Convergence	CONV1	Relative convergence criteria on objective function	0.1E-2		0.1E-9		0.1E-9	0.1E-3	
	CONV2	Absolute convergence criteria on objective function	0.1E-2		0.1E-9		0.1E-9	0.1E-3	
	GMAX	Maximum constraint violation allowed at optimum	0.1E-3		0.1E-3		0.1E-3	0.1E-3	
Soft Convergence	CONVCN	Relative criteria for change in design variables	0.1E-2		0.1E-9		0.1E-9	0.1E-4	
	CONVDV	Relative criteria for change in properties	0.1E-2		0.1E-9		0.1E-9	0.1E-4	
	CONVPR	Allowable change in the maximum constraint	0.1E-2		0.1E-9		0.1E-9	0.1E-4	
Inner Optimization	ITRMOP	Number of consecutive iterations that must satisfy the relative or absolute convergence criteria before optimization is terminated in the approximate optimization problem	2	5	2	5	2	2	5

Table 5: Structural optimization performance according to GENESIS parameter settings (5 variables Version A).

	Case 1 GENESIS Default, ITRMOP=2	**Case 2** GENESIS default, ITRMOP=5	**Case 3** Current setting, ITRMOP=2	**Case 4** Current setting, ITRMOP=5	**Case 5** Tight convergence parameters, Default move limits, ITRMOP=2
Cycles/run	7.4	11.8 (1.59×Case 1)	21.8 (2.95×Case 1)	43.3 (5.85×Case 1)	9.6 (1.30×Case 1)
CPU/run (sec)	74.4	118.2 (1.59×Case 1)	110.9 (1.49×Case 1)	275.0 (3.70×Case 1)	103.2 (1.39×Case 1)
Mean of W_b improvements w.r.t Case 1	NA	1.5%	-6.4%	1.4%	0.5%

Table 6: Results of outlier correction of Case 1
(5 variables Version A).

	B	Number of outliers *a*/*b*/*c*/*d*[*]	Mean of correction on outliers(lb)[†]	Mean of correction on inliers(lb)[‡]	Ratio of mean correction on OL to IL	% of correction to full correction[§]	RMSE in lbs (% to the mean W_b)	mean W_b	R^2
Before repair	NA	NA	NA	NA	NA	NA	3075.2 (6.5%)	47349	0.9788
IRLS repair	1.9	13/14/2/2	2940.4	486.3	6.05	44.1	2758.4 (5.9%)	47009	0.9823
NIRLS1 repair	1.9	18/19/2/2	2683.4	413.9	6.48	54.7	2741.8 (5.8%)	46927	0.9824
NIRLS2 repair	1.9	17/18/2/2	2668.2	438.6	6.08	51.5	2740.6 (5.8%)	46952	0.9825
IRLS repair	1.0	39/45/1/2	1244.6	489.4	2.54	60.1	2808.2 (6.0%)	46886	0.9817
NIRLS1 repair	1.0	36/42/2/2	1580.8	339.3	4.66	71.2	2785.5 (6.0%)	46800	0.9818
NIRLS2 repair	1.0	29/33/2/2	1723.7	412.7	4.18	61.0	2691.4 (5.7%)	46879	0.9831
Full repair[¶]	NA	NA	NA	NA	NA	100.0	2868.2 (6.2%)	46579	0.9808

*: *a*: Number of outliers successfully repaired (relative improvement is greater than 0)
b: Number of detected outliers
c: Number of big outliers detected (relative improvement is greater than 10%)
d: Total number of big outliers out of the 121 data points (relative improvement is greater than 10%)
†: (Sum of W_b correction on outliers)/*b*
‡: (Sum of W_b correction on data points other than outliers)/(Total number of points - *b*)
§: (Sum of W_b correction on outliers) / (Sum of W_b correction on all 121 points)
¶: All 121 points corrected

Table 7: Results of outlier correction of Case 3
(5 variables Version A).

	B	Number of outliers a/b/c/d[*]	Mean of correction on outliers(lb)[†]	Mean of correction on inliers(lb)[‡]	Ratio of mean correction on OL to IL	% of correction to full correction[§]	RMSE in lbs (% to the mean W_b)	Mean W_b (lbs)	R^2
Before repair	NA	NA	NA	NA	NA	NA	4782.0 (9.5%)	50365	0.9497
IRLS repair	1.9	17/19/14/33	10512	2533.3	4.15	43.6	3044.5 (6.2%)	48714	0.9795
NIRLS1 repair	1.9	15/17/13/33	11242	2567.4	4.38	41.7	3011.2 (6.2%)	48785	0.9798
NIRLS2 repair	1.9	15/17/13/33	11242	2567.4	4.38	41.7	3011.2 (6.2%)	48785	0.9798
IRLS repair	1.0	35/40/18/33	6488.6	2451.6	2.65	56.7	3520.6 (7.3%)	48220	0.9724
NIRLS1 repair	1.0	46/50/31/33	7355.3	1272.7	5.78	80.3	2912.7 (6.2%)	47325	0.9797
NIRLS2 repair	1.0	46/51/30/33	7108.3	1365.8	5.20	79.1	2817.1 (5.9%)	47369	0.9814
Full repair[¶]	NA	NA	NA	NA	NA	100.	2868.2 (6.2%)	46579	0.9808

*: *a*: Number of outliers successfully repaired (relative improvement is greater than 0)
b: Number of detected outliers
c: Number of big outliers detected (relative improvement is greater than 10%)
d: Total number of big outliers out of the 121 data points (relative improvement is greater than 10%)
†: (Sum of W_b correction on outliers)/*b*
‡: (Sum of W_b correction on data points other than outliers)/(Total number of points - *b*)
§: (Sum of W_b correction on outliers) / (Sum of W_b correction on all 121 points)
¶: All 121 points corrected

Table 8: Results of outlier correction of Case 1
(5 variables Version B).

	B	Number of outliers *a*/*b*/c/*d**	Mean of correction on outliers(lb)†	Mean of correction on inliers(lb)‡	Ratio of mean correction on OL to IL	% of correction to full correction§	RMSE in lbs (% to the mean W_b)	mean W_b	R^2
Before repair	NA	NA	NA	NA	NA	NA	4874.6 (9.5%)	51104	0.9681
IRLS repair	1.9	16/21/9/12	8235.3	1200.0	6.86	57.9	3260.0 (6.6%)	49731	0.9839
NIRLS1 repair	1.9	19/24/12/12	8484.7	934.4	9.08	68.1	3475.7 (7.0%)	49488	0.9809
NIRLS2 repair	1.9	19/24/12/12	8484.7	934.4	9.08	68.1	3475.7 (7.0%)	49488	0.9809
IRLS repair	1.0	33/43/10/12	4712.3	1160.4	4.06	67.8	3260.9 (6.6%)	49496	0.9839
NIRLS1 repair	1.0	35/45/11/12	4868.2	986.1	4.94	73.3	3022.5 (6.1%)	49365	0.9862
NIRLS2 repair	1.0	36/45/12/12	5304.7	743.6	7.13	79.9	3471.8 (7.1%)	49209	0.9810
Full repair¶	NA	NA	NA	NA	NA	100.0	3485.1 (7.2%)	48731	0.9811

*: *a*: Number of outliers successfully repaired (relative improvement is greater than 0)
b: Number of detected outliers
c: Number of big outliers detected (relative improvement is greater than 10%)
d: Total number of big outliers out of the 126 data points (relative improvement is greater than 10%)
†: (Sum of W_b correction on outliers)/*b*
‡: (Sum of W_b correction on data points other than outliers)/(Total number of points - *b*)
§: (Sum of W_b correction on outliers) / (Sum of W_b correction on all 126 points)
¶: All 126 points corrected

Table 9: Results of outlier correction of Case 7
(5 variables Version B).

	B	Number of outliers *a*/*b*/c/*d**	Mean of correction on outliers(lb)†	Mean of correction on inliers(lb)‡	Ratio of mean correction on OL to IL	% of correction to full correction§	RMSE in lbs (% to the mean W_b)	Mean W_b (lbs)	R^2
Before repair	NA	NA	NA	NA	NA	NA	4594.8 (8.7%)	53069	0.9701
IRLS repair	1.9	23/23/17/34	9020.3	3292.2	2.74	38.0	2873.1 (5.6%)	51423	0.9877
NIRLS1 repair	1.9	25/25/18/34	9658.7	3020.7	3.20	44.2	3747.3 (7.3%)	51153	0.9774
NIRLS2 repair	1.9	25/25/18/34	9658.7	3020.7	3.20	44.2	3747.3 (7.3%)	51153	0.9774
IRLS repair	1.0	46/49/21/34	5609.4	3528.6	1.59	50.3	3034.0 (6.0%)	50888	0.9865
NIRLS1 repair	1.0	43/45/28/34	7728.5	2454.1	3.15	63.6	3574.0 (7.1%)	50309	0.9796
NIRLS2 repair	1.0	43/44/29/34	8009.7	2367.5	3.38	64.5	3530.9 (7.0%)	50272	0.9801
Full repair¶	NA	NA	NA	NA	NA	100.	3485.1 (7.2%)	48731	0.9811

*: *a*: Number of outliers successfully repaired (relative improvement is greater than 0)
b: Number of detected outliers
c: Number of big outliers detected (relative improvement is greater than 10%)
d: Total number of big outliers out of the 126 data points (relative improvement is greater than 10%)
†: (Sum of W_b correction on outliers)/*b*
‡: (Sum of W_b correction on data points other than outliers)/(Total number of points - *b*)
§: (Sum of W_b correction on outliers) / (Sum of W_b correction on all 126 points)
¶: All 126 points corrected

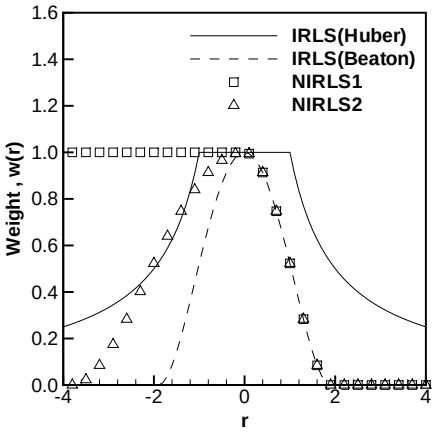

Figure 1: Various weight functions.

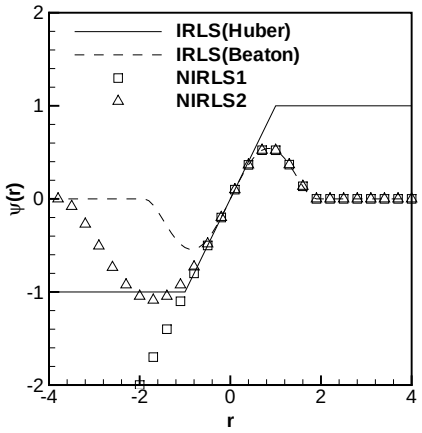

Figure 2: ψ functions.

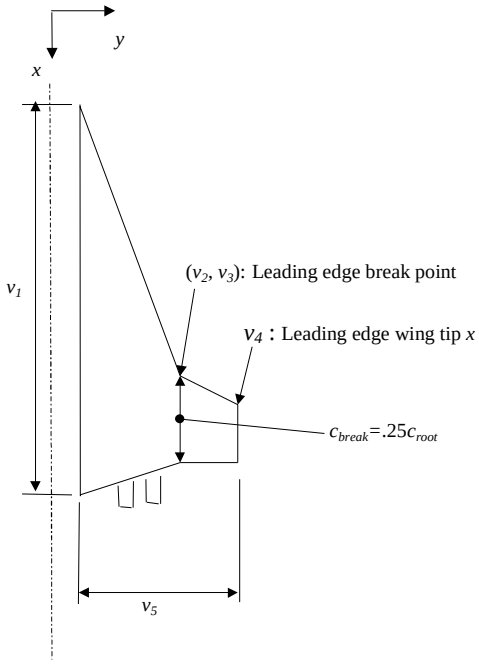

(a) 5 variable Version A.

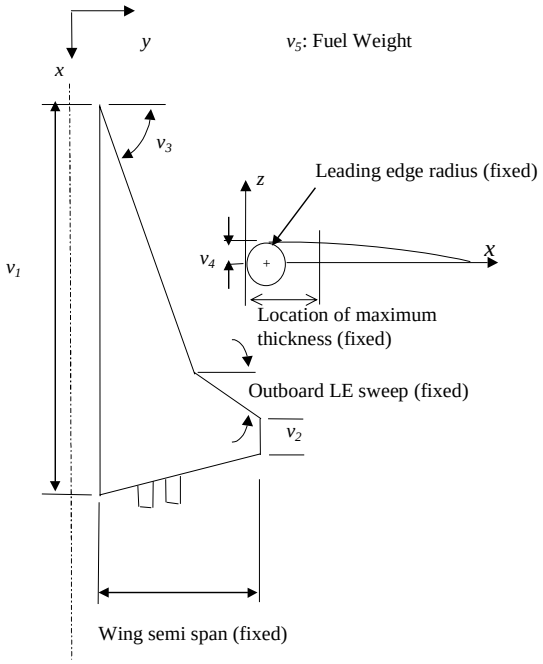

(b) 5 variable Version B.

Figure 3: Design variables in the simplified HSCT design problems.

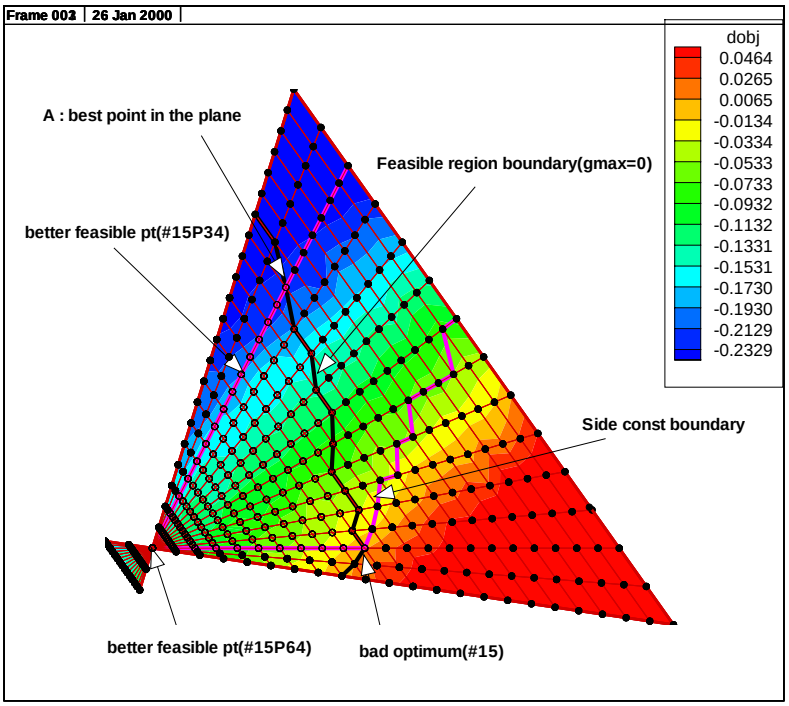

Figure 4: Contour of objective function increment and constraint boundaries on a plane through a poor computed optimum.

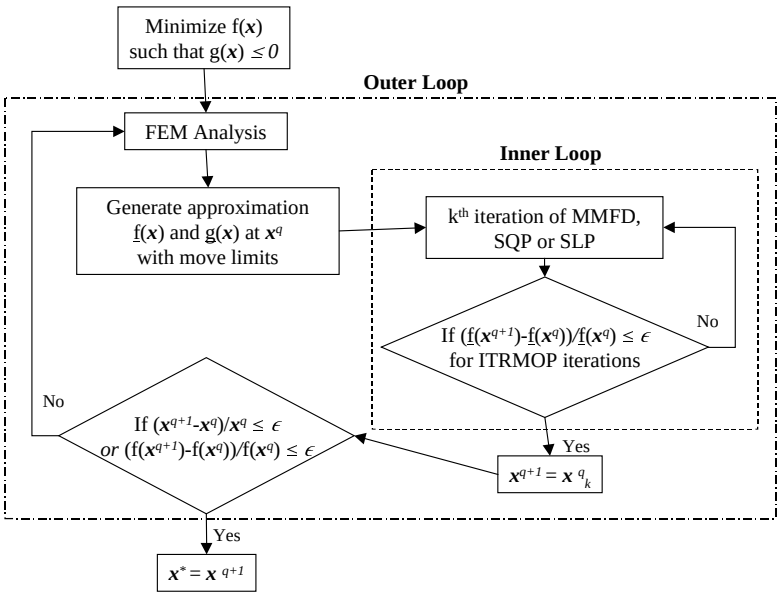

Figure 5: Structure of GENESIS structural optimization.

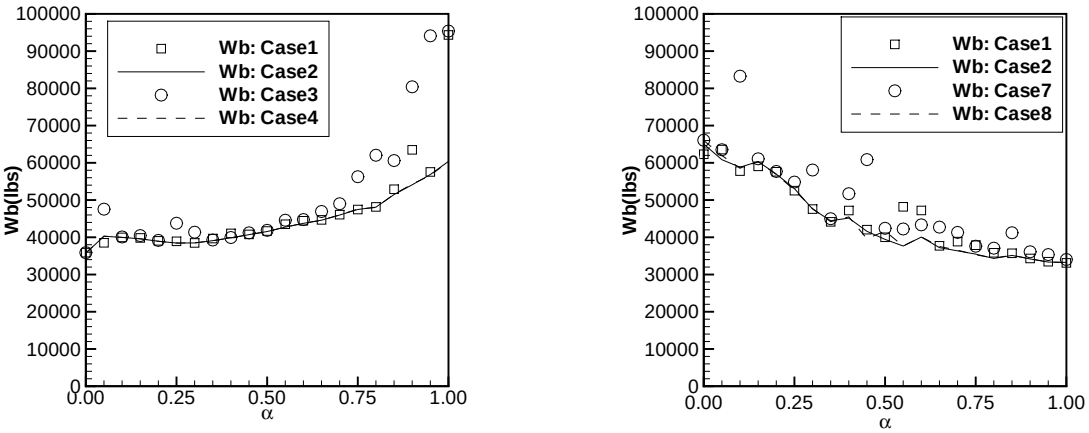

(a) 5 variable Version A.

(b) 5 variable Version B.

Figure 6: Design line plots of W_b estimation according to the parameter setups.

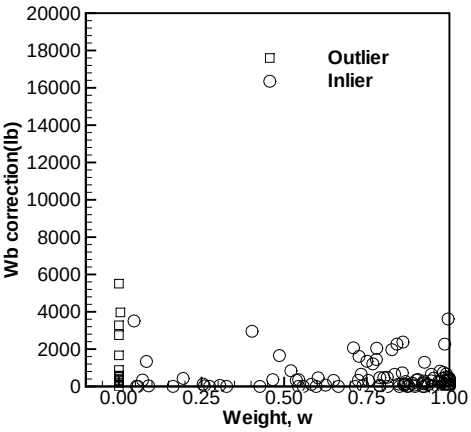

(a) IRLS, *B*=1.9.

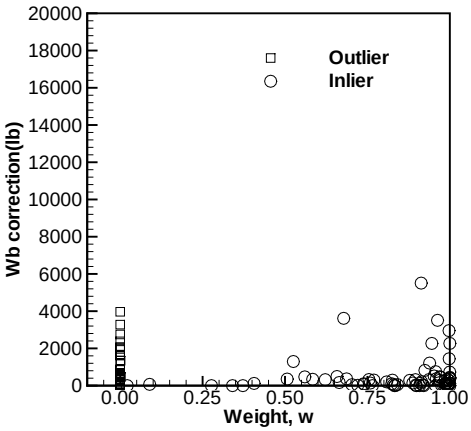

(b) IRLS, *B*=1.0.

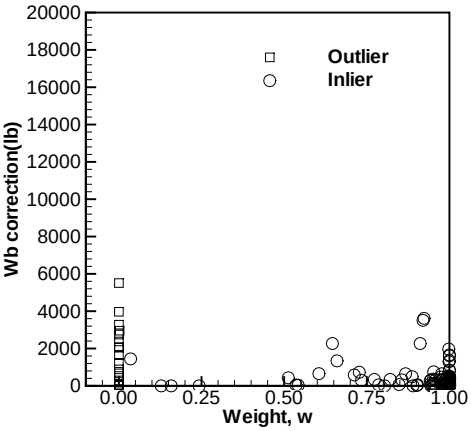

(c) NIRLS1, *B*=1.9.

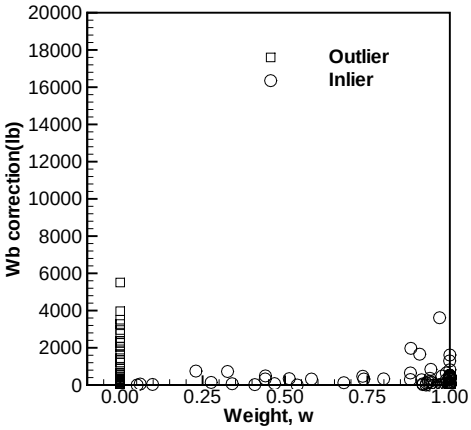

(d) NIRLS1, *B*=1.0.

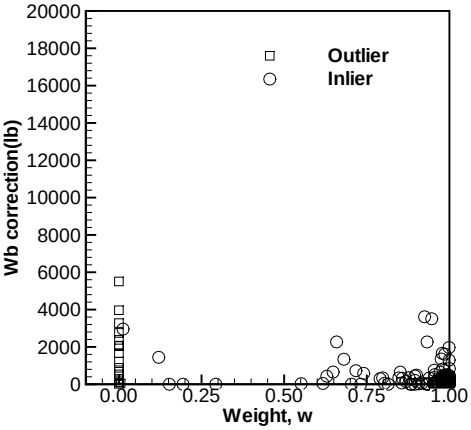

(e) NIRLS2, *B*=1.9.

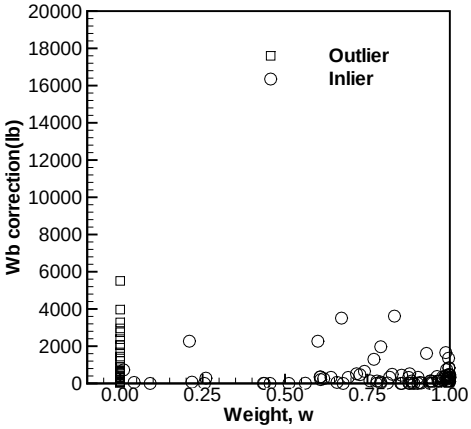

(f) NIRLS2, *B*=1.0.

Figure 7: Actual correction for the detected outliers and inliers for Case 1.

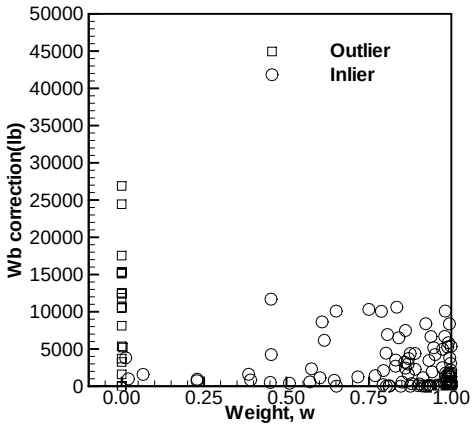

(a) IRLS, *B*=1.9.

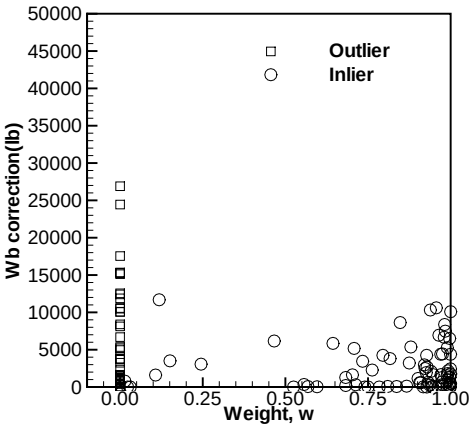

(b) IRLS, *B*=1.0.

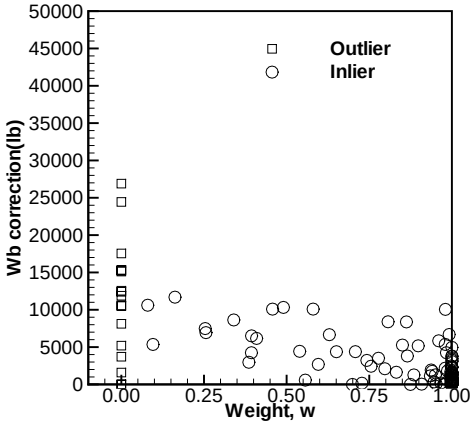

(c) NIRLS1, *B*=1.9.

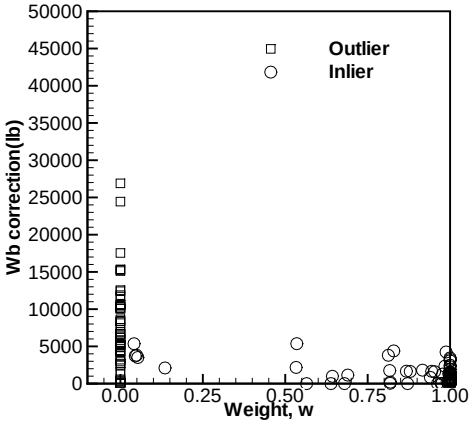

(d) NIRLS1, *B*=1.0.

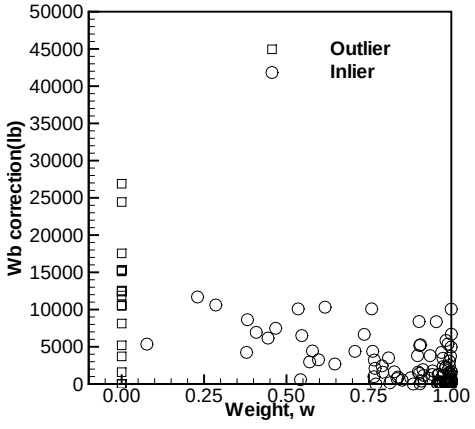

(e) NIRLS2, *B*=1.9.

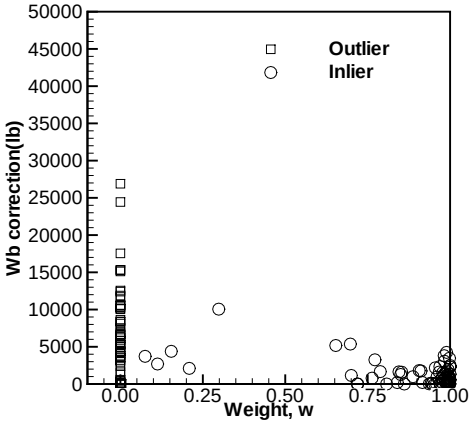

(f) NIRLS2, *B*=1.0.

Figure 8: Actual correction for the detected outliers and inliers for Case3.

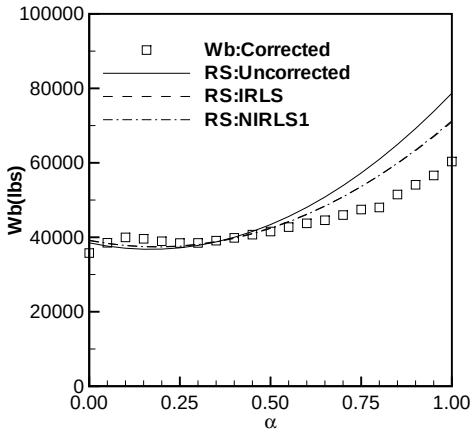

(a) Case 3 for the 5 variable Version A, B=1.9.

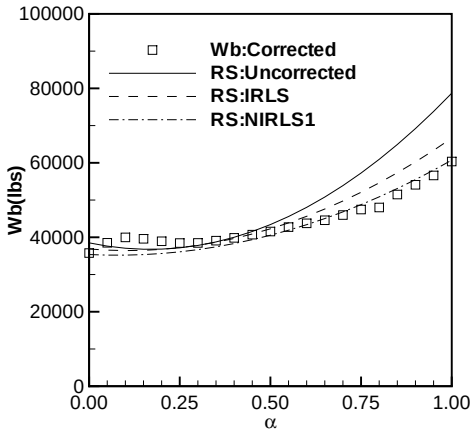

(b) Case 3 for the 5 variable Version A, B=1.0.

Figure 9: Effects of outlier correction on the W_b response surfaces.